

General method for final focus system design for circular colliders

Riccardo de Maria

CERN, Geneva, and EPFL, Lausanne, Switzerland
(Received 9 August 2007; published 31 March 2008)

Colliders use final focus systems to reduce the transverse beam sizes at the interaction point in order to increase collision event rates. The maximum focal strength (gradient) of the quadrupoles, and the maximum beam size in them, together limit the beam size reduction that is possible. The goal of a final focus system design is to find the best compromise between quadrupole aperture and quadrupole gradient, for the magnet technology that is used. This paper develops a design method that identifies the intrinsic limitations of a final focus system, validates the results of the method against realistic designs, and reports its application to the upgrade of the Large Hadron Collider final focus.

DOI: [10.1103/PhysRevSTAB.11.031001](https://doi.org/10.1103/PhysRevSTAB.11.031001)

PACS numbers: 29.27.Eg

I. INTRODUCTION

Since the appearance of the alternating focusing theory [1], there have been attempts to find systematic tools to study the effect of multiplets of quadrupolar magnets on the beam phase space. One application is the design of a final focus system [2] able to squeeze the transverse size of two particle beams in the interaction point (IP) of a collider and thereby to increase the interaction rate.

Several papers and reports have been written on this topic, see [3,4]. The results, albeit useful as calculation tools for the analysis of a layout (in particular when the computational resources were limited), are not suited for the design process of a modern IR due to the complexity of the formulas that relate the layout parameters with the performance goals.

An approach, used in particular for a linear collider by taking advantage of the symmetries in the layout and using a thin lens approximation (e.g. [5,6] and more recently [7]), allows one to optimize the chromatic and geometric aberrations by using nonlinear elements and to achieve very small spot size, but leads to longer and more complex structures compared to the ones involving only linear elements. In circular colliders, this approach has not been yet proved satisfactory due to space limitations, which does not allow efficient layouts, and to a nonexact cancellation of the aberrations, which limits the dynamic aperture (see [8]).

In recent years, the SSC (see [9]), the LHC (see [10]), and its upgrade (see [11]) triggered several studies for developing optimization tools for final focus systems. The high energy of the particles poses immediately a limit to the focusing capabilities of the superconducting magnets due to the limited peak field that superconducting cables can sustain. Those studies were therefore motivated by the importance of understanding the performance limits (namely smallest possible beam size at the IP, aberrations, aperture margins) induced by a given magnet technology, not only for estimating the potential limitations of colliders but also as a feedback for the research in the magnet technology (see [12–14]).

These studies used several approximations (e.g. thin lens approximation in [15,16]) and restricted the analysis to some particular cases (e.g. coarse parameter scan for the SSC in [17] or symmetric triplets for the LHC in [15,16,18]) in order to decrease the complexity of the equation and reduce the dimensionality of the parameter space. On the other hand, this strategy exposes the studies to the chance of missing the true optimum and does not answer the question of what limitations are induced by a magnet technology compared to the limitations of a given layout. In fact, the thin lens approximation is not always accurate and usually requires a refinement using the exact thick lens theory that spoils the generality of the results. A symmetric triplet is a layout that offers good performance close (e.g. in the nominal LHC), but not in all possible scenarios.

This article tries to overcome those limitations by introducing a simplified layout involving only quadrupoles whose performance (beam size at the IP, required peak field, chromatic aberrations) can be explored systematically.

The equations used here well approximate the exact thick lens theory. In the case of round beams at the IP, they allow one to relate the layout parameters to the performance goals through a set of univariate functions found numerically.

A similar set of functions has been found in [18] for a symmetric triplet layout, but they are valid in a limited region of parameters.

The layout provides performance close to the best possible for a given magnet technology for round beams. Although the layout is not practical as is, a small variation of parameters allows designing a realistic layout with slightly lower performance.

The performance of the layout, being close to the best possible for a given technology, allows one to link directly the limitations of a magnet technology with the limitations of a final focus system for round beams.

The optimization of a flat beam option is not covered by this paper because it relies on implementation details (e.g.

beam screen) and physical effects (e.g. beam-beam effects) that are difficult to model in a general and scalable way. Nevertheless, the strategy and the approximations presented here, being more general, could be used in such cases as well.

Section II reviews the equations for the beam size. Section III shows the approximation for the beam size equations valid in a final focus system and used throughout the article. Sections IV, V, and VI introduce simplified assumptions on the focus system in order to present a family of abstract layouts that is close to the requirements for a final focus system and whose parameters are completely solvable in terms of the designs goals. Section VII shows an application for triplets layout and finds the relation between a design goal (the peak beta function) and the design parameters (β^* , L^* , k). Section VIII compares the estimated given by the abstract layout with the actual values of existing designs. Section IX shows an application for an upgrade of the LHC interaction region identifying the limitations of possible final focus systems induced by the limits of the magnet technology.

II. EQUATION FOR THE BEAM SIZE

The purpose of a final focus system is to reduce the size of the beam as much as possible at the IP, while leaving free space for the detector.

In the paraxial approximation, the transverse coordinates x and y of a particle in a pure quadrupole field follow the Hill's equation:

$$x''(s) + k(s)x(s) = 0 \quad (1)$$

$$y''(s) - k(s)y(s) = 0, \quad (2)$$

where k is the quadrupole normalized gradient and the derivative refers to the magnet longitudinal position s . The change of the sign between the two planes shows that a quadrupole, while it is focusing in one plane, is defocusing in the other.

It is possible to determine the beam size of a monochromatic beam using the ansatz (see [1]):

$$x(s) = \sqrt{2I\beta(s)} \cos[\mu(s) + \phi], \quad (3)$$

where I and ϕ are the action and the initial phase of the particle in one plane and $\beta(s)$ and $\mu(s)$ are functions which follow the equations:

$$\frac{1}{2}\beta''(s)\beta(s) - \frac{1}{4}\beta'(s)^2 + k(s)\beta(s)^2 = 1 \quad (4)$$

$$\mu(s) = \int_{s_0}^s \frac{1}{\beta(s')} ds'. \quad (5)$$

The rms beam size σ of a beam can therefore be expressed as:

$$\sigma = \sqrt{\varepsilon\beta}, \quad (6)$$

where $\varepsilon = \langle I \rangle$ is the emittance of the beam equal to the average action of the particles and β is the amplitude function, called the beta function.

The same treatment is valid for the other transverse plane y by inverting the sign of k .

III. APPROXIMATION FOR FINAL FOCUS SYSTEMS

Starting from the IP, where β is minimal, and propagating the beta function in a field-free region where $k(s) = 0$, Eqs. (4) and (5) have the solutions:

$$\beta(s) = \beta^* + \frac{s^2}{\beta^*} \quad (7)$$

$$\mu(s) = \arctan\left(\frac{s}{\beta^*}\right) \quad (8)$$

$$\simeq \frac{\pi}{2} - \frac{\beta^*}{s} + \frac{1}{3}\left(\frac{\beta^*}{s}\right)^3 + O\left[\left(\frac{\beta^*}{s}\right)^5\right], \quad (9)$$

where $\beta^* = \beta(0)$ is the beta function at the IP.

If s is much bigger than β^* , the phase advance in this region is approximately $\frac{\pi}{2}$.

This allows one to approximate the function

$$w(s) = \sqrt{\beta(s)} \quad (10)$$

for $s \gg \beta^*$ by the trajectory of a particle with initial phase equal to $\frac{\pi}{2}$ and initial conditions:

$$x(0) = 0 \quad x'(0) = 1/\sqrt{\beta^*}. \quad (11)$$

The approximation continues to hold in the final focus system provided that $\beta(s)$ remains large with respect to the s coordinate, so that the contributions to the integral in Eq. (5) remain negligible.

In this approximation the equation for $w(s)$ is the same as for $x(s)$; that is,

$$w''(s) + k(s)w(s) = 0. \quad (12)$$

The same result can be found noting that the exact differential equation for $w(s)$ is

$$w''(s) + k(s)w(s) - \frac{1}{w^3(s)} = 0, \quad (13)$$

which is derived in [1].

In Eq. (13), the term $1/w^3$ becomes negligible if k is bigger than $1/w^4$ or w^2 is larger than the length of the focus system.

A solution of Eq. (12) for a positive and constant $k(s) = k$ is

$$w(s) = w_0 \cos(s\sqrt{k}) + \frac{w_0'}{\sqrt{k}} \sin(s\sqrt{k}) \quad (14)$$

and for a negative and constant $k(s) = -k$ is

$$w(s) = w_0 \cosh(s\sqrt{k}) + \frac{w'_0}{\sqrt{k}} \sinh(s\sqrt{k}), \quad (15)$$

where w_0 and w'_0 are the initial conditions.

A first application of the approximation (12) allows one to find the maximum β inside a focusing quadrupole. If the approximation is valid and the maximum β in a quadrupole is not trivially located in one of the two extremities, the solution of the system

$$w(s_m) = w_m = w_0 \cos(s_m\sqrt{k}) + \frac{w'_0}{\sqrt{k}} \sin(s_m\sqrt{k}) \quad (16)$$

$$w'(s_m) = 0 = -w_0\sqrt{k} \sin(s_m\sqrt{k}) + w'_0 \cos(s_m\sqrt{k}), \quad (17)$$

which is equivalent to

$$\tan(s_m\sqrt{k}) = \frac{w'_0}{w_0\sqrt{k}} = -\frac{\alpha_0}{\beta_0\sqrt{k}} \quad (18)$$

$$\beta_m = w_m^2 = w_0^2 + \left(\frac{w'_0}{\sqrt{k}}\right)^2 = \beta_0 + \frac{\alpha_0^2}{\beta_0 k} \quad (19)$$

gives the value β_m and the location s_m of the maximum β , assuming that $w_0 = \sqrt{\beta_0}$ and $w'_0 = -\alpha_0/w_0$ are the initial conditions at the beginning of the quadrupole.

An important property of systems described by a given $k(s)$ is that the solution of Eq. (12) for a given initial condition is still a solution of the differential equation after a rescaling of the type

$$w \rightarrow \alpha w, \quad (20)$$

because Eq. (12) follows a linear homogeneous equation.

Therefore all the possible solutions of a given problem depend only on one parameter $w_0 = w(0)/w'(0)$. This property can be used to scale the solutions for identical systems whose initial conditions are linearly dependent.

IV. CONSTANT GRADIENT FINAL FOCUS SYSTEM

It is possible to construct a simple layout for a final focus which can be completely solved and is already close to an optimal final focus in terms of minimum beam size for a given peak field.

The layout consists of a piecewise constant gradient which assumes only two values:

$$k(s) = \bar{k}k, \quad (21)$$

where k is a positive number and $\bar{k} = \pm 1$ for a focusing quadrupole and for a defocusing one, respectively. Figure 1 shows an example using three quadrupoles.

Using this assumption, it is possible to introduce a function $\bar{w}(\theta)$ that depends on a normalized quantity θ and is defined by the equations:

$$\theta = s\sqrt{k} \quad (22)$$

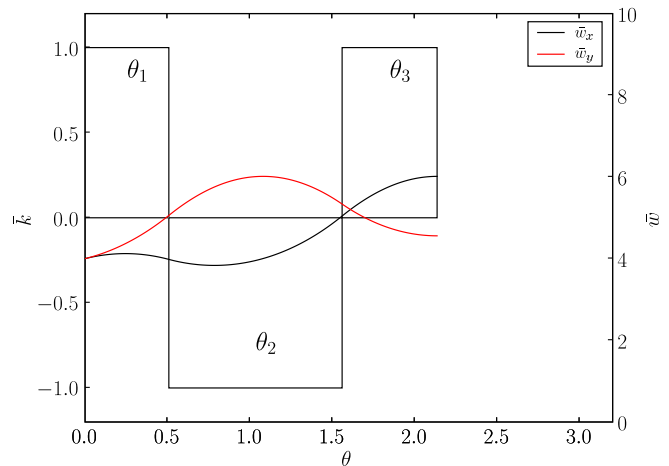


FIG. 1. (Color) Point to parallel constant gradient triplet with initial condition $\bar{w}_0 = 4$, $\bar{w}'_0 = 1$. The boxes represent the position, length, and polarity of the quadrupoles. The curves show $w = \sqrt{\beta}$ as a function of the normalized longitudinal position $\theta = s\sqrt{k}$. A scaling of the initial condition translates into scaling w while keeping the same lengths for the quadrupoles (property 1). The solution remains unchanged if $k \rightarrow \alpha k$, $\theta \rightarrow \theta/\alpha$, $w'_0 \rightarrow \alpha w'_0$.

$$w(s) = w(\theta/\sqrt{k}) \equiv \bar{w}(\theta). \quad (23)$$

The function $\bar{w}(\theta)$ follows the differential equation

$$\bar{w}''(\theta) + \bar{k} \bar{w}(\theta) = 0. \quad (24)$$

The solution can be written, respectively, for $\bar{k} = 1$ and $\bar{k} = -1$, as

$$\begin{pmatrix} \bar{w}(\theta) \\ \bar{w}'(\theta) \end{pmatrix} = R(\theta) \begin{pmatrix} \bar{w}_0 \\ \bar{w}'_0 \end{pmatrix} \quad (25)$$

$$\begin{pmatrix} \bar{w}(\theta) \\ \bar{w}'(\theta) \end{pmatrix} = H(\theta) \begin{pmatrix} \bar{w}_0 \\ \bar{w}'_0 \end{pmatrix}, \quad (26)$$

where $R(\theta)$ and $H(\theta)$ are circular and hyperbolic rotations:

$$R(\theta) = e^{\theta J} = \begin{pmatrix} \cos(\theta) & \sin(\theta) \\ -\sin(\theta) & \cos(\theta) \end{pmatrix} \quad J = \begin{pmatrix} 0 & -1 \\ 1 & 0 \end{pmatrix} \quad (27)$$

$$H(\theta) = e^{\theta S} = \begin{pmatrix} \cosh(\theta) & \sinh(\theta) \\ \sinh(\theta) & \cosh(\theta) \end{pmatrix} \quad S = \begin{pmatrix} 0 & 1 \\ 1 & 0 \end{pmatrix}. \quad (28)$$

Using these simple maps, it is possible to derive a complete system of equations that are sufficient to find the equations that allow one to find the maximum \bar{w} and the normalized lengths as a function of the initial and final conditions (see [19]).

V. SCALINGS FOR FINAL FOCUS SYSTEMS

The scaling properties of the constant gradient final focus systems allow one to optimize one layout in normalized quantities and scale the results all the parameters involved. In particular, we are interested in final focus systems that use efficiently the aperture of the quadrupoles in order to limit the peak beta function in the quadrupoles, which is a source of aberrations and sensitivity to errors, and, at the same time, to limit the lengths of the quadrupole because the particles at the edge of the beam will see the maximum bending field.

It is possible to derive the constraints that allow one to find the layout which minimizes the peak beta function and the lengths of the quadrupoles. This information represents also an intrinsic limit of the final focus system because all the variation would imply larger beta and larger lengths.

The analysis that follows is limited to a final focus system where the beta functions are equal in both plane at IP (round beams). This is the case for the final focus systems for hadron colliders like the LHC, the SSC, TEVATRON, RHIC. The initial conditions depend on only one parameter β^* and L^* which is a beta function at the IP and the distance of the first quadrupole of the focus system from the IP.

They can be written for both planes as

$$w(0) = \frac{L^*}{\sqrt{\beta^*}} \quad w'(0) = \frac{1}{\sqrt{\beta^*}}. \quad (29)$$

Therefore if we use the initial conditions in normalized coordinate

$$\bar{w}(0) = \bar{w}_0 = L^* \sqrt{k} \quad \bar{w}'(0) = 1 \quad (30)$$

and use Eq. (20), we can find the equations

$$\beta(s) = \frac{\bar{w}(s\sqrt{k})^2}{k\beta^*} \quad s = \frac{\theta}{\sqrt{k}} \quad (31)$$

which allow one to scale the quantities from normalized to not normalized values.

VI. CONSTANT GRADIENT POINT TO PARALLEL FOCUSING

It is now possible to introduce generalizing assumptions on the layout of final focus systems in order to disclose the intrinsic limitations by neglecting the practical aspects that concern only specific cases.

We first assume that the final focus system is in charge only of reducing the beam divergence to zero, thus the conditions at the end of the last quadrupole are for both planes $w' = \bar{w}' = 0$.

In order to focus a round beam, it is necessary that the focus system has equal focusing properties for both planes. Only a set of quadrupoles larger than 3 exhibits this properties. The analysis can be carried out for multiplets of any number of elements as shown in [19], but here we limit the

analysis to triplets, which have a more general interest because they result in the shortest structures.

The final focus systems that minimize the beta function in the quadrupoles are the ones for which the peaks of the beta are the same. In this case both apertures are used efficiently. For a triplet structure the number of peaks is two, as Fig. 1 shows.

Another assumption is to put no gaps between quadrupoles. The layout is not a practical final focus system as it is, but a small variation of the parameters and the addition of gaps between the quadrupoles allows it to become a realistic final focus system at the cost of an increase of the peak beta function.

The layouts that are compatibles with the mentioned assumptions have the property to be at the border between a focusing and a defocusing system while minimizing the peak beta function.

VII. TRIPLET LAYOUT

A triplet layout uses three alternating gradient quadrupoles. Figure 1 shows the triplet structure together with w_x and w_y as a function of the longitudinal coordinate s .

For a triplet layout, the previous assumptions translate in three constraints using the normalized lengths of the quadrupoles $\theta_1, \theta_2, \theta_3$ and the initial condition \bar{w}_0 as free parameters:

$$\bar{w}_m \equiv \bar{w}_{x3} = \sqrt{\bar{w}_{y1}^2 + \bar{w}'_{y1}{}^2} \quad (32)$$

$$\bar{w}'_{x3} = 0 \quad (33)$$

$$\bar{w}'_{y3} = 0, \quad (34)$$

where \bar{w}_m^2 is proportional to the beta peak in the triplets and

$$\begin{pmatrix} \bar{w}_{y1} \\ \bar{w}'_{y1} \end{pmatrix} = H(\theta_1) \begin{pmatrix} \bar{w}_0 \\ 1 \end{pmatrix} \quad (35)$$

$$\begin{pmatrix} \bar{w}_{y3} \\ \bar{w}'_{y3} \end{pmatrix} = H(\theta_3)R(\theta_2)H(\theta_1) \begin{pmatrix} \bar{w}_0 \\ 1 \end{pmatrix} \quad (36)$$

$$\begin{pmatrix} \bar{w}_{x3} \\ \bar{w}'_{x3} \end{pmatrix} = R(\theta_3)H(\theta_2)R(\theta_1) \begin{pmatrix} \bar{w}_0 \\ 1 \end{pmatrix}. \quad (37)$$

It is possible to use the constraints to eliminate the $\theta_1, \theta_2, \theta_3$ and write $\bar{w}_m, \theta_1, \theta_2, \theta_3$ as a function of \bar{w}_0 . Figure 2 shows the functions $\bar{w}_m(\bar{w}_0), \theta_1(\bar{w}_0), \theta_2(\bar{w}_0), \theta_3(\bar{w}_0)$ computed numerically.

For $\bar{w}_m(\bar{w}_0)$ it is possible to find a good fit:

$$\bar{w}_m(\bar{w}_0) \simeq 2 + 1.11e^{-\bar{w}_0} + \bar{w}_0, \quad (38)$$

which gives a smaller error of 1% for \bar{w}_0 ranging from 0 to 50.

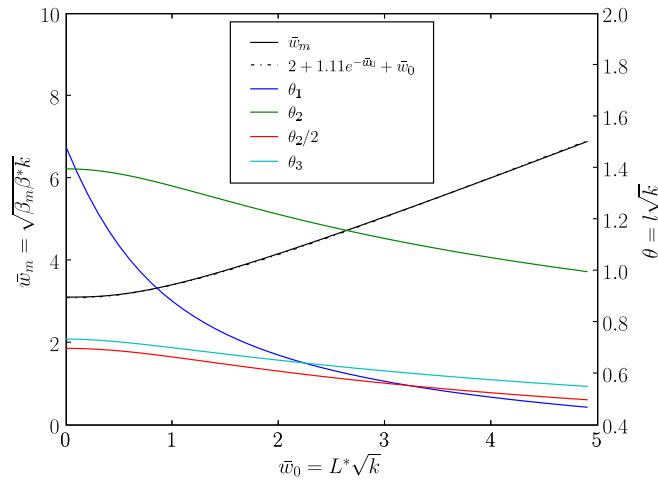


FIG. 2. (Color) Solution for a triplet final focus system. The figure shows the normalized lengths $\theta_i = l_i \sqrt{k}$ and the maximum $w = \sqrt{\beta}$ as a function of the initial conditions parameterized according to $w = L^* \sqrt{k}$, $w' = 1$. The solution can be scaled to any β^* , L^* , k according to the equations shown in the labeling of the axis. Values for the θ_1 , $\theta_2/2$, θ_3 have similar values, which is why is sometimes convenient to use quadrupoles of the same length to reduce the complexity of the final focus system at the cost of suboptimal performance.

Using Eq. (31), the maximum beta function for constant gradient point to parallel final focus system is given by

$$\beta_m(\beta^*, L^*, k) \simeq \frac{(2 + 1.11 e^{-L^* \sqrt{k}} + L^* \sqrt{k})^2}{k \beta^*}. \quad (39)$$

The system can be extended to any multiplet. A quadruplet shows a slightly smaller peak of w but a larger overall length as compared to the triplet solution. The quintuplet shows no improvement in terms of beam size compared to the previous solution, while increasing the number of magnetic elements. A larger number of elements follow this trend; the only effect is to progressively reduce the difference between w_x and w_y which is in most of the case an unwanted feature.

TABLE I. Parameters of final focus systems in existing designs. The first four columns show β^* , L^* , and the largest normalized strengths for the real designs. The fifth column estimates the minimum beta peak in the triplet using Eq. (39). Real designs show always larger values for the beta peak with respect to the minimum possible because of the gaps between the quadrupoles, short focal lengths (the estimates assume infinite focal length for the triplet), and not optimized structures. The last columns show the quadrupoles filling ratio using $\sum_{\text{quads}} |k| l / \sum_{\text{all}} l$ and an equivalent minimum beta peak computed using the normalized gradient scaled with the filling ratio in order to take into account the presence of gaps. Using the equivalent quadrupole strengths, the estimates are closer but always smaller or equal to the actual values. Data justifies the assumption that constant gradient point to parallel focusing systems can be used to estimate the properties of real final focus systems without the need of a complete design.

	β^* [m]	L^* [m]	Maximum k [m ⁻²]	β_m [m]	Minimum β_m [m]	Filling ratio	Equivalent k [m ⁻²]	Equivalent β_m [m]
LHC	0.550	22.96	0.008 72	4425	3809	0.782	0.006 82	4401
Scaled LHC	0.250	22.96	0.008 72	9733	8379	0.782	0.006 82	9683
RHIC	0.700	25.36	0.057 73	1906	1622	0.649	0.037 47	1824
SSC	0.500	20.00	0.003 34	8029	7357	0.927	0.003 10	7810
TEVATRON	0.355	7.62	0.041 92	1108	966	0.872	0.036 57	1062

The previous results show that the first quadrupole has always the smallest beam size. At the cost of a specialized magnet with a smaller aperture and a larger gradient but with the same pole field ($\propto wk$), it is possible to push the performance a bit further.

VIII. ESTIMATES FOR EXISTING DESIGNS

Colliders like RHIC, TEVATRON, SSC and the LHC (see [10,20–22], respectively) use triplets as final focus systems. Table I shows the parameters of their final focus systems and justifies the hypothesis of the method presented in this paper.

The beta peaks of the existing designs are always larger than the minimum peak given by Eq. (39) because of the presence of gaps between the quadrupoles, the short focal length [Eq. (39) assume infinite focal length for the triplet assembly] and finally simplified structures.

The gaps are usually necessary to provide room for the interconnections (can be long for superconducting magnets) and corrector magnets. A short focal length is usually required for matching the beam size in the final focus system with the requirements of the rest of the machine (e.g. arc cells). Simplified structures are used, for instance, for reducing the number of magnet types in the final focus system (usually two like in TEVATRON and the LHC as opposed to three like in RHIC, SSC and the triplet presented in this paper) and recover the flexibility by adjusting the gradient of the quadrupoles or the gap lengths between the quadrupoles.

Nevertheless realistic structures present beta peaks close to the minimum values which can be used as realistic and good estimates without requiring a complete design.

IX. ESTIMATES FOR THE LHC UPGRADE

As soon as the LHC reaches its nominal performance, the present triplet magnets will be close to their performance limit. An upgrade of the interaction region (IR)

together with a better understanding of the machine will be required for a further increase of the LHC performance (see [12–14,23]).

Using the results from the previous chapter, we can systematically explore the options for an upgrade using the existing NbTi technology and the new Nb₃Sn technology. In the following, we will use the results of the previous chapter together with some empirical estimates to draw a region in the parameter space compatible with the technology and operation limits of the LHC.

A. Focus limit

As shown previously, constant gradient gapless final focus systems give a good estimate of the minimum beta function that a final focus can achieve with a given quadrupole gradient and β^* .

We can use Eq. (39) and the curves in Fig. 2 for finding a first guess to the parameters of the final focus system that optimize the compactness and the beta peak.

Choosing a value for L^* and β^* (e.g. $L^* = 23$ m and 0.25 m for the case of the LHC upgrade), it is possible to show (see Fig. 3) the region of the parameters gradient and peak beta function for which a constant gradient triplet can focus a round beam in both planes. In other words, from this plot it is possible to estimate which is the minimum gradient needed to design a final focusing system which features a given peak of the beta function. In fact, the necessary variations, for transforming the limit case in a realistic design (i.e. positive focal length, gaps between quadrupoles), have the effect of increasing the peak beta function. Such an increase can be partially recovered by optimizing the first quadrupole.

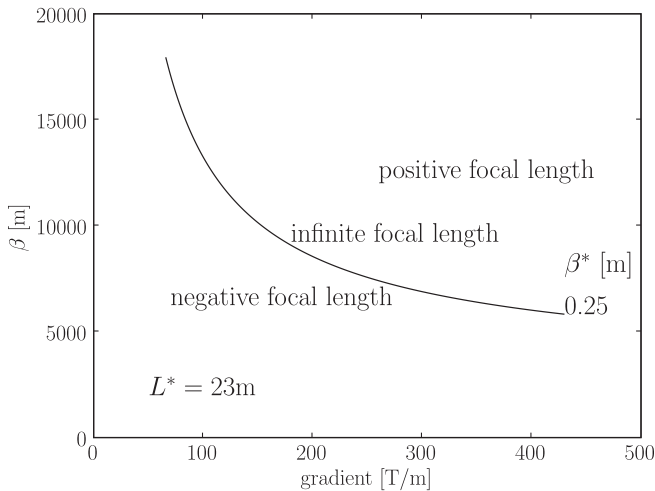


FIG. 3. Focus limit. The figure shows the region in the (maximum β , gradient) space, where it is possible to find a solution for a triplet final focus system for the LHC given $L^* = 23$ m and $\beta = 25$ cm. The upper area indicates the parameters of a triplet that can focus in both planes. The curve shows the minimal β peak for a constant gradient focus system as a function of the gradient.

B. Aperture limit

The apertures of quadrupole magnets are limited by the field gradient (see [24]). Aperture d and gradient g are roughly related by

$$d = 2 \frac{B_p}{g}, \quad (40)$$

where B_p is the magnetic field that saturates the iron yoke ($B_p \approx 2$ T for iron) for normal conducting magnets or the peak field in the coil compatible with the critical surface, temperature, and current of the superconducting coils (e.g. $B_p \approx 7.5$ T for NbTi coils or $B_p \approx 12$ T for Nb₃Sn coils, refined values can be found in [25]) for superconducting magnets.

The aperture of the quadrupoles needs to be as large as required by the size of the beam (or two beams as in the LHC interaction region or TEVATRON). The aperture of the beam can be given in terms of multiples of σ and fixed quantities that take into account the thickness of the items in vacuum chambers (e.g. beam pipe, beam screen, cryogenic pipes) and tolerances. In the case of two beams circulating in the same vacuum chamber, a separation (usually given in multiples of σ) is needed to reduce the cross talks that distort the beam dynamics (beam beam effect see [26]).

In the LHC the two beams must be separated by 10σ , one from the other and from the walls of the vacuum chamber. It is possible to give a crude estimate of the required transverse mechanical aperture in the quadrupoles including tolerances using

$$d > 33\sigma + 22 \text{ mm}, \quad (41)$$

where d is the inner coil diameter, σ is the rms beam size, and 22 mm is an empirical quantity which takes the mechanical tolerances of the magnet and the closed orbit, the beam screen, and the beam pipe into account (see [27]).

Using the estimates for the maximum β in the triplet Eqs. (39), (6), and (40), and choosing a value for B_p , it is possible to draw the lines that delimit the region of parameters compatible with a given magnet technology.

Figure 4 shows two lines (red) for different values of B_p compatible with NbTi and Nb₃Sn, respectively. The region below the red lines is compatible with the indicated peak field because the beta peak and thus the beam size is smaller than the aperture of the magnet.

C. Aberration limit

The aberrations reduce the size of the part of beam which is stable after many turns. They are proportional to some power of the beta function and may depend in a nontrivial way on the field quality of the magnet. It is difficult to find an empirical law which sets a limit for the beta function and field quality. Experience shows that for the LHC one reaches the limits for the chromaticity correction with a beta function larger than 18 km in the

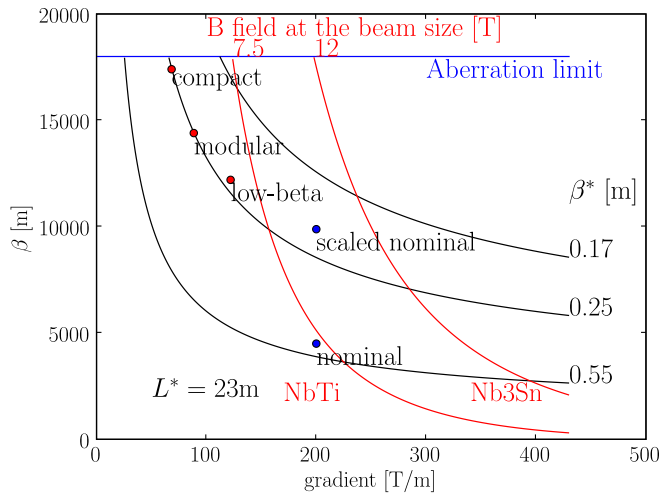


FIG. 4. (Color) LHC upgrade. The figure shows the region in the maximum (beta, gradient) space, where it is possible to find a solution for a triplet final focus system for the LHC. The region above the gray lines (focus limit) and below the red (aperture limit) and blue (aberration limit) show the region of parameters compatible with a given magnet technology (e.g. NbTi and Nb₃Sn) with a pole field of about 7.5 and 12 T. The points represent some realistic upgrade layouts presented in [27] and the nominal LHC.

final focus magnets and observes severe limitations on the dynamic aperture (see [8,28]).

Figure 4 shows therefore a limiting line (blue) at 18 km.

D. Parameter space

All previous estimates define the region in the parameter space for a realistic final focus (regions above the black lines and below the blue and red lines in Fig. 4). Figure 4 shows in addition the matched optics presented in [27] and the nominal optics. One can see how their parameters fit the ones predicted by the method although the matched optics does not strictly use the same layout. Figure 4 shows that keeping the same layout for the triplet requires a magnet with a larger peak field (e.g. using Nb₃Sn coils), but layouts compatible with the nominal technology exist and require smaller gradients than the nominal layout.

X. CONCLUSIONS

A constant gradient point to parallel final focus is a simple model whose parameters can be found for any initial conditions through a set of functions of one parameter. These functions are the solutions of a system of equations that can be solved numerically and can be used as a design tool.

The approximation and properties stated so far are always valid for a final focus system and allow one to write simpler conditions compared to the exact theory.

A realistic implementation of the layouts can be derived including the necessary gaps between the quadrupoles.

This will change the layout parameters and increases the maximum beta, total length, and chromaticity. As long as the gap lengths are smaller than the magnet lengths, the effect is small if the integrated strengths are kept constant. A comparison between the estimates and existing designs shows agreement and justifies the assumptions.

The method and the results can be used for exploring systematically the expected performance of a final focus system for which the pole field of the magnet is one of the limitations. In addition, the method determines the layout parameter such as length, position, and gradient of the magnets.

The analysis was concluded for the case of the LHC in the framework of the LHC IR upgrade studies. The conditions for an effective final focus system are combined with the constraints coming from the magnet technology and the LHC machine parameters. The results show the set of layout parameters compatible with the NbTi or Nb₃Sn technology and the expected performance. The predictions are compared with several realistic designs showing a good agreement with the analysis.

ACKNOWLEDGMENTS

I am grateful to Oliver Bruening for encouraging me to study this topic and the initial discussion, and to Steve Peggs and Stephane Fartoukh for suggesting I use the simplified differential equation for ν [Eq. (12)]. I would like to thank Massimo Giovannozzi, Werner Herr, Ulrich Dorda, and Leonid Rivkin for the patient review of this paper. I acknowledge the support of the European Community-Research Infrastructure Activity under the FP6 “Structuring the European Research Area” program (CARE, Contract No. RII3-CT-2003-506395).

- [1] E. D. Courant and H. S. Snyder, *Ann. Phys. (Leipzig)* **3**, 1 (1958).
- [2] K. Robinson and G. Voss, Technical Report No. CEAL-TM-149, CEA, 1965.
- [3] E. Regenstreif, CERN Report No. CERN 67-6, 1967, <http://doc.cern.ch/yellowrep/1967/1967-006/p1.pdf>.
- [4] E. Regenstreif, CERN Report No. CERN 67-8, 1967, <http://doc.cern.ch/yellowrep/1967/1967-008/p1.pdf>.
- [5] K.L. Brown and R.V. Servranckx, SLAC Technical Report No. SLAC-PUB-3381, 1984, <http://www.slac.stanford.edu/pubs/slacpubs/3000/slac-pub-3381.html>.
- [6] K.L. Brown and R.V. Servranckx, *Nucl. Instrum. Methods Phys. Res., Sect. A* **258**, 480 (1987).
- [7] P. Raimondi and A. Seryi, *Phys. Rev. Lett.* **86**, 3779 (2001).
- [8] R. de Maria, O. Bruening, and P. Raimondi, at the European Particle Accelerator Conference EPAC’06, Edinburgh, Scotland, UK, 2006 (CERN Technical Report No. CERN-LHC-Project-Report-934, 2006), <http://doc.cern.ch/archive/electronic/cern/preprints/lhc/lhc-project-report-934.pdf>.

- [9] J. Jackson, R. Barton, and R. Donaldson, SSC Central Design Group Technical Report No. SSC-SR-2020, 1986.
- [10] O. Bruening, P. Collier, P. Lebrun, S. Myers, R. Ostojic, J. Poole, and P. Proudlock, CERN Technical Report No. CERN-2004-003, 2004, <http://ab-div.web.cern.ch/ab-div/Publications/LHC-DesignReport.html>.
- [11] O. S. Bruening *et al.*, CERN Technical Report No. LHC-Project-Report-626, 2002, <http://cdsweb.cern.ch/search.py?recid=601847>.
- [12] F. Ruggiero, W. Scandale, and F. Zimmermann, CERN Report No. CERN-2005-006, 2004.
- [13] F. Ruggiero, W. Scandale, and F. Zimmermann, CERN Report No. CERN-2006-008, 2005.
- [14] W. Scandale, T. Taylor, and F. Zimmermann, CERN Report No. CERN-2007-002, 2006.
- [15] E. T. d'Amico and G. Guignard, CERN Report No. CLIC-Note 341, 1997, <http://doc.cern.ch/archive/electronic/cern/preprints/ps/ps-97-025.pdf>.
- [16] E. d'Amico and G. Guignard, CERN Report No. CERN-SL 98-014, 1998, <http://doc.cern.ch/archive/electronic/cern/preprints/sl/sl-98-014.pdf>.
- [17] S. Peggs, in SSC Summer Study (1984).
- [18] J. P. Koutchouk, L. Rossi, and E. Todesco, CERN Report No. lhc-project-report 1000, 2007, <http://doc.cern.ch/archive/electronic/cern/preprints/lhc/lhc-project-report-1000.pdf>.
- [19] R. de Maria, CERN Report No. LHC-Report 1051, 2007, <http://doc.cern.ch/archive/electronic/cern/preprints/lhc/lhc-project-report-1051.pdf>.
- [20] Rhic Design Manual (2000), <http://www.agsrhichome.bnl.gov/NT-share/rhicdm>.
- [21] Tevatron Official Lattice (2008), http://www-ap.fnal.gov/~martens/tev_lattice/tev_lattice.html.
- [22] E. Courant, A. Garren, D. Johnson, and K. Steffen, Report No. SSC N-139, 1986, <http://lss.fnal.gov/archive/other/ssc/ssc-n-139.pdf>.
- [23] F. Ruggiero, O. Bruening, R. Ostojic, L. Rossi, W. Scandale, T. Taylor, and A. Devred, in EPAC04, 2004.
- [24] S. Russenschuck, Report No. CERN-2006-002, 2006.
- [25] L. Rossi and E. Todesco, Phys. Rev. ST Accel. Beams **9**, 102401 (2006).
- [26] W. Herr, Report No. CERN-2006-002, 2006.
- [27] O. Bruening, R. de Maria, and R. Ostojic, CERN Report No. LHC-Report 1008, 2007, <http://doc.cern.ch/archive/electronic/cern/preprints/lhc/lhc-project-report-1008.pdf>.
- [28] R. de Maria and O. Bruening, CERN Technical Report No. CERN-LHC-Project-Report-933, 2006, <http://doc.cern.ch/archive/electronic/cern/preprints/lhc/lhc-project-report-933.pdf>.